Theory of the 2S-2P Lamb shift and 2S hyperfine splitting in muonic hydrogen

Aldo Antognini,[1,*] Franz Kottmann,[1] François Biraben,[2]

Paul Indelicato,[2] François Nez,[2] and Randolf Pohl[3]

[1]*Institute for Particle Physics, ETH Zurich, 8093 Zurich, Switzerland.*

[2]*Laboratoire Kastler Brossel, École Normale Supérieure,*

CNRS and Université P. et M. Curie, 75252 Paris, CEDEX 05, France.

[3]*Max–Planck–Institut für Quantenoptik, 85748 Garching, Germany.*

The 7σ discrepancy between the proton rms charge radius from muonic hydrogen and the CODATA-2010 value from hydrogen spectroscopy and electron-scattering has caused considerable discussions. Here, we review the theory of the 2S-2P Lamb shift and 2S hyperfine splitting in muonic hydrogen combining the published contributions and theoretical approaches. The prediction of these quantities is necessary for the determination of both proton charge and Zemach radii from the two 2S-2P transition frequencies measured in muonic hydrogen [1, 2].

I. INTRODUCTION

The study of energy levels in hydrogen [3, 4], hydrogen-like atoms like muonium [5] or positronium [6], as well as free [7] and bound [8] electron g-factors provide the most accurate and precise verifications of quantum electrodynamics (QED) [9].

Comparison of the measured transition frequencies in hydrogen with theory is limited by the uncertainty of the proton structure [9, 10]. Here, the main uncertainty originates from the root mean square (rms) charge radius of the proton, defined as $r_{\mathrm{E}}^2 = \int \mathrm{d}^3 r \, r^2 \rho(\boldsymbol{r})$, where ρ is the normalized charge density of the proton. Muonium and positronium are made from point-like elementary particles and therefore do not suffer from uncertainties due to finite-size effects. The ultimate experimental precision is however limited by the short lifetime of these systems. A way out to improve the test of hydrogen energy levels is given by spectroscopy of muonic hydrogen (μp), an atom formed by a muon and a proton. This provides a precise determination of r_{E}.

Recently the comparison of the measured $2\mathrm{P}_{3/2}^{F=2} - 2\mathrm{S}_{1/2}^{F=1}$ transition in muonic hydrogen [1]

$$\Delta E_{2\mathrm{P}_{3/2}^{F=2}-2\mathrm{S}_{1/2}^{F=1}}^{\mathrm{exp}} = 206.2949(32) \ \mathrm{meV} \tag{1}$$

with the theoretical prediction based on bound-state QED [11–13], as summarized in the Supplementary Information of [1], from now on referred to as Ref. [14]

$$\Delta E_{2\mathrm{P}_{3/2}^{F=2}-2\mathrm{S}_{1/2}^{F=1}}^{\mathrm{th}} = 209.9779(49) - 5.2262 \, r_{\mathrm{E}}^2 + 0.0347 \, r_{\mathrm{E}}^3 \quad \mathrm{meV} \tag{2}$$

---

*Electronic address: aldo@phys.ethz.ch

yielded $r_E = 0.84184(67)$ fm [1]. Throughout the paper we assume radii to be in fm, resulting energies in meV.

The muonic hydrogen value of r_E is an order of magnitude more precise than the CODATA-2010 value $r_E^{\text{CODATA}} = 0.8775(51)$ fm [15] which originates from a least-square adjustment of measurements from hydrogen spectroscopy[3, 4, 16–21] and electron-proton scattering [22–24]. However, the muonic hydrogen value is 4% smaller than the CODATA value [15]. This 7 standard deviations discrepancy is now commonly referred to as the "proton radius puzzle" [25].

Many efforts have been made to solve the radius puzzle. Theory of muonic hydrogen energy levels has been refined significantly, and is reviewed here. The suggestion [26] that molecular effects due to $p\mu e^-$ ion formation may be responsible for the discrepancy has been ruled out recently [27]. Electron scattering has seen a huge activity recently, both from new measurements [24, 28, 29] and new re-analyses of the world data [30–39]. Several authors studied proton structure at low energies [40–48]. Also, physics beyond the standard model has been considered [26, 49–58]. On the experimental side, several projects aim at a new determination of the Rydberg constant (R_∞) at MPQ, LKB [21], NPL [59] and NIST [60], to rule out possible systematics shifts in the previous measurements that determine R_∞ [61]. A new measurement of the classical 2S-2P Lamb shift in hydrogen is being prepared [62]. New electron scattering measurements are proposed or under-way [63–67]. And finally, new measurements of muonic hydrogem deuterium or helium ions may in futire shed new light on the proton radius puzzle [68, 69]. Several studies have been concerned with the theory of the $n = 2$ energy levels in muonic hydrogen. Here we summarize the various contributions of these investigations updating the theoretical prediction of the muonic hydrogen 2S-2P Lamb shift and 2S-HFS. We anticipate already here that no big error or additional contribution have been found which could solve the observed discrepancy between experiment and theory of the 2S-2P energy difference:

$$\text{discrepancy} = \Delta E^{\text{exp}}_{2P_{3/2}^{F=2}-2S_{1/2}^{F=1}} - \Delta E^{\text{th}}_{2P_{3/2}^{F=2}-2S_{1/2}^{F=1}}(r_E^{\text{CODATA}}) = 0.31\,\text{meV}. \tag{3}$$

This corresponds to a relative discrepancy of 0.15 %.

Two transition frequencies in muonic hydrogen have been measured. One starts from the 2S-triplet state $\nu_t = 2P_{3/2}^{F=2} - 2S_{1/2}^{F=1}$ [1, 2], and the other from the 2S-singlet state $\nu_s = 2P_{3/2}^{F=1} - 2S_{1/2}^{F=0}$ [2], as shown in Fig. 1. As detailed in Sec. II we can deduce from these measurements both the "pure" Lamb shift ($\Delta E_L = \Delta E_{2P_{1/2}-2S_{1/2}}$) and the 2S-HFS splitting (ΔE_{HFS}), each independent of the other. Comparing the experimentally determined ΔE_L with its theoretical prediction given in Sec. III yields an improved r_E value free of uncertainty from the 2S-HFS. Similarly, comparing the experimentally determined ΔE_{HFS} with its theoretical prediction given in Sec. IV results in the determination of the Zemach radius r_Z.

Perturbation theory is used to calculate the various corrections to the energy levels involving an expansion of both operators and wave functions. The radiative (QED) corrections are obtained in an expansion in α, binding effects and relativistic effects in $(Z\alpha)$, and recoil corrections in the ratio of the masses of the two-body system (m/M). $Z = 1$ is the atomic charge number and α the fine structure constant. The contributions related to the proton structure are in part described by

an expansion in powers of r_E and r_Z. The book-keeping of all the corrections contributing to the μp Lamb shift and 2S-HFS is challenging because:

- All corrections are mixed as $\alpha^x \, (Z\alpha)^y \, (m/M)^z \, r_E^t$.

- There are large finite-size and recoil ($m/M \approx 1/9$) corrections.

- One cannot develop the calculation in a systematic way like in $g - 2$ for free particles.

- Widely different scales are involved: the masses, the three-momenta and the kinetic energies of the constituents.

- Different authors use different terminologies for identical terms.

- Different methods are being used: Schrödinger equation + Breit corrections versus Dirac equation, Grotch- versus Breit-type recoil corrections, all-order versus perturbative in $(Z\alpha)$ and finite-size, non-relativistic QED (NRQED) etc.

In this study we summarize all known terms included in the Lamb shift and the 2S-HFS predictions which are used in [2] to determine the proton charge radius and the Zemach radius. The majority of these terms can be found in the works of Pachucki [11, 12], Borie [13], and Martynenko [70, 71]. These earlier works have been reviewed in Eides et al.[72, 73]. After the publication of [1], a number of authors have revisited the theory in muonic hydrogen, e.g. Jentschura [74, 75], Karshenboim *et al.* [76] and Borie [77]. Note that the arXiv version 1103.1772v6 of Borie's article [77] contains corrections to the published version, which is why we refer to "Borie-v6" here. In addition Indelicato [78] checked and improved many of the relevant terms by performing numerical integration of the Dirac equation with finite-size Coulomb and Uehling potentials. Carroll *et al.* started a similar effort [79].

II.   THE EXPERIMENTAL LAMB SHIFT AND 2S-HFS

The 2S and 2P energy levels in muonic hydrogen are presented in Fig. 1. Because the measurements of the Lamb shift involve only $n = 2$ states, the main term of the binding energy (632 eV given by the Bohr structure) drops out and the results do not depend on the Rydberg constant.

The 2S-2P splitting arises from relativistic, hyperfine, radiative, recoil, and nuclear structure effects. The Lamb shift is dominated by the one-loop electron-positron vacuum polarization of 205 meV. The experimental uncertainty of the Lamb shift is of relative order $u_r \approx 10^{-5}$. Thus the various contributions to the Lamb shift should be calculated to better than ~ 0.001 meV to be able to exploit the full experimental accuracy.
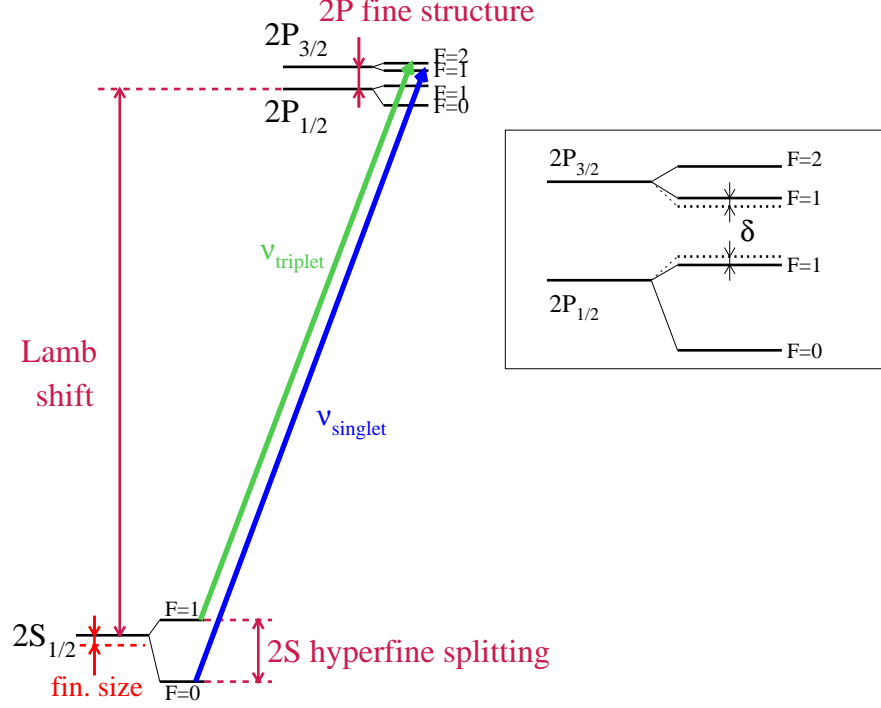
FIG. 1: 2S and 2P energy levels. The measured transitions ν_t [1] and ν_s [2] are indicated together with Lamb shift, fine and hyperfine splittings and finite-size effects. The main figure is drawn to scale. The insets zooms in on the 2P states. Here, the mixing of the 2P(F=1) levels shifts them by $\pm\delta$ (see Eq.(7)).

The two measured transition frequencies shown in Fig. 1 are given by

$$
\begin{aligned}
h\nu_t =& E(2\mathrm{P}_{3/2}^{F=2}) - E(2\mathrm{S}_{1/2}^{F=1}) \\
=& \Delta E_\mathrm{L} + \Delta E_\mathrm{FS} + \frac{3}{8}\Delta E_\mathrm{HFS}^{2\mathrm{P}_{3/2}} - \frac{1}{4}\Delta E_\mathrm{HFS},
\end{aligned}
$$

(4)

$$
\begin{aligned}
h\nu_s =& E(2\mathrm{P}_{3/2}^{F=1}) - E(2\mathrm{S}_{1/2}^{F=0}) \\
=& \Delta E_\mathrm{L} + \Delta E_\mathrm{FS} - \frac{5}{8}\Delta E_\mathrm{HFS}^{2\mathrm{P}_{3/2}} + \delta + \frac{3}{4}\Delta E_\mathrm{HFS},
\end{aligned}
$$

where h is the Planck constant, and $\Delta E_\mathrm{FS} = \Delta E_{2\mathrm{P}_{3/2}} - \Delta E_{2\mathrm{P}_{1/2}}$ is the fine structure splitting of the 2P-state. For the 2P fine structure splitting we use the value [71]

$$\Delta E_\mathrm{FS} = 8.352082 \text{ meV}, \tag{5}$$

which is in agreement with the values $8.3521\,\mathrm{meV}$ [77] and $8.351988 - 0.000052\,r_\mathrm{E}^2 = 8.351944\,\mathrm{meV}$ [78], Eq. (120). The $2\mathrm{P}_{3/2}$ hyperfine structure splitting is [71]

$$\Delta E_\mathrm{HFS}^{2\mathrm{P}_{3/2}} = 3.392588 \text{ meV}, \tag{6}$$

in agreement with $3.392511\,\mathrm{meV}$ [80]. The $2\mathrm{P}_{3/2}^{F=1}$ level is shifted upwards due to state mixing [81] of the two 2P(F=1) levels by [71]

$$\delta = 0.14456 \text{ meV} \tag{7}$$

as shown in Fig. 1. The values given in Table 8 of [77] include this shift and deviate by less than $0.0002\,\mathrm{meV}$ from the values in Eqs. (6) and (7).

ΔE_L and ΔE_HFS can be deduced independently of each other from

$$
\begin{aligned}
\frac{1}{4}h\nu_s + \frac{3}{4}h\nu_t &= \Delta E_\mathrm{L} + \Delta E_\mathrm{FS} + \frac{1}{8}\Delta E_\mathrm{HFS}^{2\mathrm{P}_{3/2}} + \frac{1}{4}\delta \\
&= \Delta E_\mathrm{L} + 8.8123(2) \text{ meV}
\end{aligned}
$$

$$
\begin{aligned}
h\nu_s - h\nu_t &= \Delta E_\mathrm{HFS} - \Delta E_\mathrm{HFS}^{2\mathrm{P}_{3/2}} + \delta \\
&= \Delta E_\mathrm{HFS} - 3.2480(2) \text{ meV}
\end{aligned}
$$

(8)

where the uncertainties of the constant terms correspond to uncalculated higher-order QED terms, and differences between the various authors. These uncertainties are small compared to both the uncertainties of the measured transition frequencies [2] and the uncertainties of the theoretical prediction for ΔE_L and ΔE_HFS (see below).

Finite-size effects are small for the 2P states but have been included in the theoretical prediction of both the fine and hyperfine contributions. For the fine splitting they have been computed perturbatively to be $-0.0000519\,r_\mathrm{E}^2 = -0.00004$ meV [77] and with an all-order approach $-0.0000521\,r_\mathrm{E}^2 = -0.00004$ meV [78]. The finite-size contributions to the $2\mathrm{P}_{3/2}$ hyperfine splitting are $< 10^{-5}$ meV [78]. Hence the finite-size related uncertainties of the constant terms in Eqs. (8) are negligible at the present level of experimental accuracy.

III.   THE LAMB SHIFT PREDICTION AND THE PROTON CHARGE RADIUS

The main contribution to the Lamb shift in muonic hydrogen is given by the one-loop electron-positron vacuum polarization (eVP). The second largest term is due to the finite extension of the proton charge and is proportional to $m_r^3\,r_\mathrm{E}^2$, where $m_r \approx 186m_e$ is the reduced mass of the μp system and m_e the electron mass. The third largest contribution is given by the Källén-Sabry (two-loop eVP) diagrams. The fourth largest term is the muon one-loop self-energy summed with the one-loop muon-antimuon vacuum polarization (μVP).

In has to be stressed that the observed discrepancy (Eq. 3) is larger than any contribution except for the four terms listed above. Therefore a solution of the proton radius puzzle in the context of muonic hydrogen theory could arise either from one-loop VP, or proton structure effects, or fundamental problems in bound-state QED, but hardly from a missing or wrong higher-order contribution. Nevertheless it is necessary to compute all these higher order contributions to better than ~ 0.001 meV in order to exploit the accuracy of the measurements and to determine r_E with a relative accuracy of $u_r \approx 3 \times 10^{-4}$, which corresponds to 0.0003 fm. The radiative, relativistic, binding and recoil corrections to ΔE_L are summarized in Table I, whereas the proton-structure dependent contributions to ΔE_L are given in Table II.

A. Proton structure independent contributions

The corrections to the energy levels predicted by the Schrödinger equation solved for the point-charge Coulomb potential are usually calculated using perturbation theory. Relativistic corrections are obtained from the two-body Breit-Hamiltonian. To check the validity of the perturbative approach the largest contribution (one-loop eVP) has been recalculated by numerical integration of the Dirac equation [77–79, 82]. The inclusion of the Uehling term to the Coulomb potential yields the relativistic all-order one-loop eVP correction given by the sum of items #3 (205.02821 meV) and #5 (0.15102 meV) in Table I. This compares well with the perturbative results: #1 (205.0074 meV) and the corrections for relativistic and eVP iterations given by #2 (0.018759 meV) and #5 (0.1507 meV). Item #5 is the energy shift in second order perturbation theory related to the wave function distortion caused by one-loop eVP. Item #7 is a similar correction to the Källén-Sabry contribution. Both originate from the wave function distortion caused by one-loop eVP.

The relativistic eVP correction with the full reduced mass dependence was given in [75]. It amounts to 0.018759 meV. Karshenboim *et al.* found [76]. why this differs from the previous result of 0.0169 meV given in item #2: The previous work had been done in different gauges, and in some of those gauges some contributions (retardation and two-photon-exchange effects) had been forgotten. In #19 we give the difference between the full expansion in (m/M) of the relativistic eVP correction (Eq. (4) in [76]) and its lowest order (Eq. (6) in [76]): $E_{\rm VP}^{\rm (rel)}(2{\rm P}_{1/2}-2{\rm S}_{1/2})-E_{\rm VP}^{(0)}(2{\rm P}_{1/2}-2{\rm S}_{1/2}) = 0.018759 - 0.020843 = -0.002084$ meV. If one includes these corrections, the various approaches for the one-loop eVP contributions with relativistic-recoil corrections are consistent: Pachucki, who starts from the Schrödinger equation, becomes $205.0074+0.018759 = 205.0262$ meV. Borie, who starts from the Dirac equation, becomes $205.0282 - 0.002084 = 205.0261$ meV.

Item #11, the muon self-energy correction to eVP of order $\alpha^2(Z\alpha)^4$, was improved as summarized in Eq. (27) of [83]. It includes contributions beyond the logarithmic term with modification of the Bethe logarithm to the Uehling potential.

Item #12, eVP loop in self-energy, is part of #21 as can be seen from Fig. 22 in [84]. Thus it had erroneously been double-counted in Ref. [14] (i.e. Ref. [1]).

B. Proton structure dependent contributions

We first present the background required to understand the individual proton structure dependent contributions summarized in Table II. The main contribution due to finite nuclear size has been given analytically to order $(Z\alpha)^6$ by Friar [94]. The main result is [77]

$$\Delta E_{\rm finite\ size} = -\frac{2\pi\alpha}{3}|\Psi(0)|^2 \left[\langle r^2 \rangle - \frac{Z\alpha}{2}\, m_r\, R_{(2)}^3 + (Z\alpha)^2 \left(F_{\rm REL} + m_r^2 F_{\rm NREL} \right) \right] \tag{9}$$

TABLE I: All known radius-**independent** contributions to the Lamb shift in μp from different authors, and the one we selected (usually the all-order calculations which we consider more complete). Values are in meV. The entry # in the first column refers to Table 1 in Ref. [14]. The "finite-size to relativistic recoil correction" (entry #18 in [14]) which depends on the proton structure has been shifted to Table II, together with the small terms #26 and #27, and the proton polarizability term #25.

SE: self-energy, VP: vacuum polarization, LBL: light-by-light scattering, Rel: relativistic, NR: non-relativistic, RC: recoil correction.

#	Contribution	Pachucki [11, 12]	Nature [14]	Borie-v6 [77]	Indelicato [78]	Our choice	Ref.
1	NR one-loop electron VP (eVP)	205.0074					
2	Rel. corr. (Breit-Pauli)	0.0169[a]					
3	Rel. one-loop eVP		205.0282	205.0282	205.02821	205.02821	[78] Eq.(54)
19	Rel. RC to eVP, $\alpha(Z\alpha)^4$	(incl. in #2)[b]	−0.0041	−0.0041		−0.00208[c]	[75, 76]
4	Two-loop eVP (Källén-Sabry)	1.5079	1.5081	1.5081	1.50810	1.50810	[78] Eq.(57)
5	One-loop eVP in 2-Coulomb lines $\alpha^2(Z\alpha)^5$	0.1509	0.1509	0.1507	0.15102	0.15102	[78] Eq.(60)
7	eVP corr. to Källén-Sabry	0.0023	0.00223	0.00223	0.00215	0.00215	[78] Eq.(62), [85]
6	NR three-loop eVP	0.0053	0.00529	0.00529		0.00529	[85, 86]
9	Wichmann-Kroll, "1:3" LBL		−0.00103	−0.00102	−0.00102	−0.00102	[78] Eq.(64), [87]
10	Virtual Delbrück, "2:2" LBL		0.00135	0.00115		0.00115	[72, 87]
new	"3:1" LBL			−0.00102		−0.00102	[87]
20	μSE and μVP	−0.6677	−0.66770	−0.66788	−0.66761	−0.66761	[78] Eqs.(72)+(76)
11	Muon SE corr. to eVP $\alpha^2(Z\alpha)^4$	−0.005(1)	−0.00500	−0.004924[d]		−0.00254	[83] Eq.(29a)[e]
12	eVP loop in self-energy $\alpha^2(Z\alpha)^4$	−0.001	−0.00150			[f]	[72, 88–90]
21	Higher-order corr. to μSE and μVP		−0.00169	−0.00171[g]		−0.00171	[84] Eq.(177)
13	Mixed eVP+μVP		0.00007	0.00007		0.00007	[72]
new	eVP and μVP in two Coulomb lines				0.00005	0.00005	[78] Eq.(78)
14	Hadronic VP $\alpha(Z\alpha)^4 m_r$	0.0113(3)	0.01077(38)	0.011(1)		0.01121(44)	[91–93]
15	Hadronic VP $\alpha(Z\alpha)^5 m_r$		0.000047			0.000047	[92, 93]
16	Rad corr. to hadronic VP		−0.000015			−0.000015	[92, 93]
17	Recoil corr.	0.0575	0.05750	0.0575	0.05747	0.05747	[78] Eq.(88)
22	Rel. RC $(Z\alpha)^5$	−0.045	−0.04497	−0.04497	−0.04497	−0.04497	[78] Eq.(88), [72]
23	Rel. RC $(Z\alpha)^6$	0.0003	0.00030		0.0002475	0.0002475	[78] Eq.(86)+Tab.II
new	Rad. (only eVP) RC $\alpha(Z\alpha)^5$					0.000136	[83] Eq.(64a)
24	Rad. RC $\alpha(Z\alpha)^n$ (proton SE)	−0.0099	−0.00960	−0.0100		−0.01080(100)	[43][h] [72]
	Sum	206.0312	206.02915	206.02862		206.03339(109)	

[a]This value has been recalculated to be 0.018759 meV [75].

[b]This correction is not necessary here because in #2 the Breit-Pauli contribution has been calculated using a Coulomb potential modified by eVP.

[c]Difference between Eq. (6) and (4) in [76]: $E_{VP}^{(rel)}(2P_{1/2} - 2S_{1/2}) - E_{VP}^{(0)}(2P_{1/2} - 2S_{1/2}) = 0.018759 - 0.020843 = -0.002084$ meV (see also Table IV). Using these corrected values, the various approaches are consistent. Pachucki becomes $205.0074 + 0.018759 = 205.0262$ meV and Borie $205.0282 - 0.0020843 = 205.0261$ meV.

[d]In Appendix C, incomplete.

[e]Eq. (27) in [83] includes contributions beyond the logarithmic term with modification of the Bethe logarithm to the Uehling potential. The factor 10/9 should be replaced by 5/6.

[f]This term is part of #22, see Fig. 22 in [84].

[g]Borie includes wave function corrections calculated in [85]. The actual difference between Ref. [14] and Borie-v6 [77] is given by the inclusion of the Källén-Sabry correction with muon loop.

[h]This was calculated in the framework of NRQED. It is related to the definition of the proton radius.

with

$$F_{\text{REL}} = -\langle r^2 \rangle \left[\gamma - \frac{35}{16} + \ln(Z\alpha) + \langle \ln(m_r r) \rangle \right] - \frac{1}{3} \langle r^3 \rangle \langle \frac{1}{r} \rangle + I_2^{\text{REL}} + I_3^{\text{REL}}$$

$$F_{\text{NREL}} = \frac{2}{3} (\langle r^2 \rangle)^2 \left[\gamma - \frac{5}{6} + \ln(Z\alpha) \right] + \frac{2}{3} \langle r^2 \rangle \langle r^2 \ln(m_r r) \rangle - \frac{\langle r^4 \rangle}{40} + \langle r^3 \rangle \langle r \rangle \qquad (10)$$
$$+ \frac{1}{9} \langle r^5 \rangle \langle \frac{1}{r} \rangle + I_2^{\text{NREL}} + I_3^{\text{NREL}}$$

where $\langle r^n \rangle = \int \mathrm{d}^3 r \, r^n \rho(\boldsymbol{r})$ is the nth moment of the charge distribution, $r_{\text{E}} = \sqrt{\langle r^2 \rangle} \approx 0.84$ fm is the rms charge radius, $R_{(2)}^3$ the third Zemach moment (see below), m_r the reduced mass, γ the Euler's constant, and I_2^{NREL}, I_3^{NREL}, I_2^{REL} and I_3^{REL} are integrals which depend on the charge distributions [94].

1. One-photon exchange contribution

The coefficient $b_a = -\frac{2\pi\alpha}{3} |\Psi(0)|^2$ of the first term in Eq. (9) describes the leading finite-size effect (for the sake of comparison we follow the notation b_x given in Table B.14 of [77]). For the 2S state $b_a = -5.1973$ meV/fm^2 [77] calculated using the Schrödinger wave function Ψ.

Relativistic corrections to the finite-size effect are accounted for in F_{REL}. The coefficient proportional to $\langle r^2 \rangle$ in F_{REL} is

$$b_c = \frac{2\pi\alpha}{3} |\Psi(0)|^2 (Z\alpha)^2 \left[\gamma - \frac{35}{16} + \ln(Z\alpha) \right]. \qquad (11)$$

For the 2S-state $b_c = -0.00181$ meV/fm^2. The total one-photon exchange contribution in this then given by

$$\Delta E_{\text{OPE}} = b_a + b_c = -5.1973 \langle r^2 \rangle - 0.00181 \langle r^2 \rangle \text{ meV} = -5.1991 \langle r^2 \rangle \text{ meV}. \qquad (12)$$

The complete, relativistic, all-order calculations [78] obtain

$$\Delta E_{\text{OPE}} = -5.1994 \langle r^2 \rangle \text{ meV} \qquad (13)$$

which we will use (see Tab. II). For the 2P$_{1/2}$ state the corresponding finite size terms amount to -0.0000519 meV/fm^2 [77].

2. Third Zemach moment contribution

The second term in Eq. (9) amounts to

$$\Delta E_{\text{third Zemach}} = 0.0091 R_{(2)}^3 \text{ meV}. \qquad (14)$$

This is the second largest finite-size effect and it depends on the third Zemach moment

$$R_{(2)}^3 = \int \mathrm{d}^3 r \int \mathrm{d}^3 r' \, r^3 \, \rho_E(\boldsymbol{r} - \boldsymbol{r}') \rho_E(\boldsymbol{r}') \qquad (15)$$

which can be determined experimentally from the electric Sachs form factor G_E measured in elastic electron-proton scattering as [95]

$$R_{(2)}^3 = \frac{48}{\pi} \int \frac{dQ}{Q^4} [G_E^2(Q^2) - 1 + \frac{1}{3}Q^2\langle r^2\rangle] \,.$$ (16)

Commonly used values are $R_{(2)}^3 = 2.71(13)$ fm^3 [95] and $R_{(2)}^3 = 2.85(8)$ fm^3 [28]. It is customary [12, 77, 78] to express the third Zemach moment using the second moment of the charge distribution as

$$R_{(2)}^3 = f\langle r^2\rangle^{3/2}$$ (17)

where f is a constant which depends on the model for the shape of the proton. For an exponential charge distribution (dipole form factor) $f = 3.79$. For a Gaussian distribution $f = 3.47$. Values extracted from the measured electric form factors are $f = 3.78(31)$ [95] and $f = 4.18(13)$ [28].

Adopting $f = 4.0(2)$ from Ref. [77] to account for the spread of the various values measured in scattering experiments, one gets from Eq. (14) and Eq. (17)

$$\Delta E_{\text{third Zemach}} = 0.0365(18)\langle r^2\rangle^{3/2} \text{ meV}$$ (18)

(see first column in Table II).

A solution of the proton radius puzzle assuming a large tail of the proton charge distribution resulting in an extremely large $R_{(2)}^3$ value [96, 97], and hence a large value of f, has been ruled out by electron-proton scattering data [28, 30, 95] and by chiral perturbation theory [40, 98].

The third Zemach contribution may be seen simplistically as a second-order correction in perturbation theory given by the modification of the wave function caused by the finite size. In a quantum field framework it is part of the two-photon exchange diagrams [11, 40, 74, 99].

3. Two-photon exchange contributions

The two-photon contributions with finite-size are usually divided into an elastic part, where the intermediate virtual proton remains on-shell, and an inelastic part (proton polarizability contribution ΔE_{pol}), where the virtual proton is off-shell. The elastic part is approximately given by the $R_{(2)}^3$ term in Eq. (9).

A unified treatment of such contributions can be achieved in modern quantum field theory using the doubly-virtual Compton amplitude which can be related to measured form factors and spin averaged structure functions using dispersion relations. Part of a subtraction term needed to remove a divergence in one Compton amplitude is usually approximated using the one-photon on-shell form factor [12]. A possible large uncertainty related to this approximation has been emphasized by Miller *et al.* [42] as well as Hill and Paz [43]. However, Birse and McGovern calculated this subtraction term in the framework of heavy baryon chiral perturbation theory [46]. They obtain a contribution of $\Delta E_{\text{sub}} = -0.0042(10)$ meV, in agreement with [11, 12, 99, 100]. This value is about two orders of magnitude smaller than the discrepancy.

The total two-photon exchange contribution with finite-size amounts to [12, 46, 74, 99]

$$\Delta E_{\text{TPE}} = 0.0332(20) \text{ meV}. \tag{19}$$

It results from the sum of an elastic part $\Delta E_{\text{el}} = 0.0295(16)$ meV [46, 99], a non-pole term $\Delta E_{\text{np}} = -0.0048$ meV [46, 99], the subtraction term $\Delta E_{\text{sub}} = -0.0042(10)$ meV [46] and an inelastic (proton polarizability) contribution $\Delta E_{\text{pol}} = 0.0127(5)$ meV [99]. Additional contributions from "new models" for the "off-shell" form factor [101] have been limited to < 0.001 meV by quasi-elastic electron scattering [46]. The uncertainty of ΔE_{el} accounts for various measured form factors (Kelly [102], AMT [103] and Mainz 2010 [24, 41]). The sum

$$\Delta E_{\text{el}} + \Delta E_{\text{np}} = 0.0247(16) \text{ meV} \tag{20}$$

should be compared to $\Delta E_{\text{third Zemach}}$ corrected for recoil corrections [74] which reduce the third Zemach contribution by a factor $(0.018 \text{ meV})/(0.021 \text{ meV})$ [11] to

$$\Delta E_{\text{third Zemach+recoil}} \approx \frac{0.018}{0.021} \cdot 0.0091 R_{(2)}^3 = 0.0217(15) \text{ meV}. \tag{21}$$

The uncertainty arises from the recoil corrections $(18/21 = 0.86(4))$ and the use of $R_{(2)}^3 = 2.78(14)$ fm^3 obtained from the spreads of the values in [28, 95]. Comparison between Eq. (20) and Eq. (21) shows that there is fair agreement between the results from Eq. (9) and the more advanced quantum field theoretical approach via Compton scattering and dispersion relations described above. The approximate scaling of $0.018/0.021$ has been discussed by Jentschura [74] based on Pachucki [11], to account for recoil corrections which are automatically included in the unified treatment of the two-photon exchange contribution ΔE_{TPE}. This recoil correction to two-photon finite-size contributions is ~ -0.003 meV, much less and of opposite sign compared to the term of 0.013 meV (#18 in Table II) given by Borie who follows Friar.

4. Higher-order moments of the charge distribution

The sum of all terms in Eq. (9) beyond $\langle r^2 \rangle$ and $R_{(2)}^3$, which have been calculated assuming an exponential charge distribution and $r_E = 0.875$ fm, affects the Lamb shift by $\Delta E_{\text{finite size}}^{\text{ho, Borie}} = -0.000123$ meV [77]. Even though the assumption of an exponential distribution may not be completely realistic for these higher-order contributions, this is sufficient [77]. The smallness of this term may be qualitatively understood in a perturbative framework (Eq. (9)): higher moments of the charge distribution are always scaled by higher powers of $(Z\alpha)$.

The dependence of the $\langle r^2 \rangle$ coefficient on the assumed proton charge distribution has been shown to be weak [13, 82]. This was demonstrated by numerical integration of the Dirac equation using various proton charge distributions: exponential, Gaussian and Yukawa (see Table II). Indelicato [78] determined the total finite-size effect, also by numerical integration of the Dirac equation, using a dipole charge distribution (Eq. (44) in [78])

$$\begin{aligned}
\Delta E_{\text{finite size}} = &-5.19937 r_E{}^2 + 0.03466 r_E{}^3 + 0.00007 r_E{}^4 \\
&-0.000017 r_E{}^5 + 1.2 \cdot 10^{-6} r_E{}^6 + 0.00027 r_E^2 \log(r_E) \text{ meV}.
\end{aligned} \tag{22}$$

TABLE II: Proton structure dependent contributions to the Lamb shift in μp from different authors, and the one we selected (usually the all-order calculations which we consider more complete). Values are in meV, $\langle r^2 \rangle$ in fm^2. The entry # in the first column refers to Table 1 in Ref. [14] supplementary informations [1]. Entry # 18 is under debate.

TPE: two-photon exchange, VP: vacuum polarization, SE: self-energy, Rel: relativistic.

#	Contribution	Borie-v6 [77]	Karshenboim [76]	Pachucki [11, 12]	Indelicato [78]	Carroll [82]	Our choice
	Non-rel. finite-size	$-5.1973\langle r^2\rangle$	$-5.1975\langle r^2\rangle$	$-5.1975\langle r^2\rangle$			
	Rel. corr. to non-rel. finite size	$-0.0018\langle r^2\rangle$		-0.0009 meV^a			
	Rel. finite-size						
	exponential				$-5.1994\langle r^2\rangle$	$-5.2001\langle r^2\rangle$	$-5.1994\langle r^2\rangle$
	Yukawa					$-5.2000\langle r^2\rangle$	
	Gaussian					$-5.2001\langle r^2\rangle$	
	Finite size corr. to one-loop eVP	$-0.0110\langle r^2\rangle$	$-0.0110\langle r^2\rangle$	$-0.010\langle r^2\rangle$	$-0.0282\langle r^2\rangle$		$-0.0282\langle r^2\rangle$
	Finite size to one-loop eVP-it.	$-0.0165\langle r^2\rangle$	$-0.0170\langle r^2\rangle$	$-0.017\langle r^2\rangle$	(incl. in -0.0282)		
	Finite-size corr. to Källén-Sabry	^{b}			$-0.0002\langle r^2\rangle$		$-0.0002\langle r^2\rangle$
new	Finite size corr. to μ self-energy	(0.00699) ^{c}			$0.0008\langle r^2\rangle$		$0.0009(3)\langle r^2\rangle^d$
	ΔE_{TPE} [46]						$0.0332(20)$ meV
	elastic (third Zemach)^e						
	measured $R^3_{(2)}$	$0.0365(18)\langle r^2\rangle^{3/2}$					(incl. above)
	exponential			$0.0363\langle r^2\rangle^{3/2}$	$0.0353\langle r^2\rangle^{3/2\,f}$	$0.0353\langle r^2\rangle^{3/2}$	
	Yukawa					$0.0378\langle r^2\rangle^{3/2}$	
	Gaussian					$0.0323\langle r^2\rangle^{3/2}$	
25	inelastic (polarizability)	$0.0129(5)$ meV [99]		$0.012(2)$ meV			(incl. above)
new	Rad. corr. to TPE	$-0.00062\langle r^2\rangle$					$-0.00062\langle r^2\rangle$
26	eVP corr. to polarizability						0.00019 meV [93]
27	SE corr. to polarizability						-0.00001 meV [93]
18	Finite-size to rel. recoil corr.	$(0.013$ meV$)$ ^{g}		^{h}			(incl. in ΔE_{TPE})
	Higher-order finite-size corr.	-0.000123 meV			$0.00001(10)$ meV		$0.00001(10)$ meV
	2P$_{1/2}$ finite-size corr.	$-0.0000519\langle r^2\rangle$ ^{i}			(incl. above)	(incl. above)	(incl. above)

^{a}Corresponds to Eq. (6) in [12] which accounts only for the main terms in F_{REL} and F_{NREL}.

^{b}This contribution has been accounted already in both the -0.0110 meV/fm^2 and -0.0165 meV/fm^2 coefficients.

^{c}Given only in Appendix C. Bethe logarithm is not included.

^{d}This uncertainty accounts for the difference between all-order in $Z\alpha$ and perturbative approaches [80].

^{e}Corresponds to Eq. (20).

^{f}This value is slightly different from Eq. (22) because here an all-order in finite-size AND an all-order in eVP approach was used.

^{g}See Appendix F of [94]. This term is under debate.

^{h}Included in ΔE_{TPE}. This correction of $0.018 - 0.021 = -0.003$ meV is given by Eq. (64) in [11] and Eq. (25) in [12]. This correction is also discussed in [74] where the 6/7 factor results from 0.018/0.021.

^{i}Eq. (6a) in [77].

Equation (22) was attained by fitting the eigenvalues of the Dirac equation obtained for a finite-size Coulomb potential for various values of the proton charge radius. Hence, it accounts for all-order finite-size effects.

The first coefficient of this equation is in agreement with $b_a + b_c = -5.1973 - 0.00181 = -5.1991$ meV/fm^2 of [77] and the second one is compatible with Eq. (18). This implies that the two approaches, one starting from the Dirac equation with finite-size-corrected Coulomb potential, and the other one starting from the Schrödinger solution (with point-like Coulomb potential) complemented with relativistic and finite-size corrections, are equivalent. The sum of the terms of Eq. (22) beyond r_{E}^2 and r_{E}^3 is only ~ 0.00004 meV, suggesting that the higher moments of the charge distribution do not affect significantly the prediction of the muonic hydrogen Lamb shift.

Sick [95] showed that $R^3_{(2)}$ extracted from the integral of Eq. (16) applied at the world data is most sensitive to the cross sections measured at $Q^2 \approx 0.05$ (GeV/c)^2. Higher Q^2 data contributes, too [97], but $R^3_{(2)}$ is rather insensitive to the lowest Q^2 region. Therefore $R^3_{(2)}$ cannot be dramatically increased by contributions from very low Q^2, where no data is available [30].

The theoretical prediction of the finite-size terms given in Eq. (9) could potentially become problematic if the higher moments of the charge distribution $\langle r^4 \rangle$, $\langle r^5 \rangle$, $\langle r^6 \rangle$ and $\langle r^2 \rangle \langle \log r \rangle$ etc. were large. However, these moments have been evaluated using electron-scattering data [28] down to the lowest experimentally accessible exchanged photon momentum of $Q^2_{\min} = 0.004$ (GeV/c)^2. The values reported in [28] are small suggesting that the finite-size effect in muonic hydrogen is properly described by the $\langle r^2 \rangle$ and $R^3_{(2)}$ terms alone.

Extending De Rújula's argument [96, 97], scattering experiments cannot completely exclude the existence of a "thorn" or a "lump" in the form factor $G_E(Q^2)$ at extremely low-Q^2 regime [104] which could give rise to unexpectedly large higher moments of the charge distribution. Nevertheless, such a low-Q^2 behaviour is disfavoured by chiral perturbation theory (χPT) and vector meson dominance (VMD) models [47] which account for the pion cloud in the low-energy regime. It was demonstrated by Pineda that $R^3_{(2)}$ is about 2-3 fm^3 in the leading chiral expansion term [40, 98]. This sets tight constraints on the long tail of the proton charge distribution. Still it is important to further investigate the proton structure at very low Q^2 with various techniques from χPT, to lattice QCD and VMD.

5. Radiative and higher-order corrections to the finite-size effect

Radiative corrections to the finite-size contributions are listed in Table II. Using a perturbative approach Borie calculated the finite-size correction to one-loop eVP ($-0.0110\langle r^2 \rangle$ meV), the finite-size correction to one-loop eVP-iteration ($-0.0165\langle r^2 \rangle$ meV) and the radiative-correction to two-photon exchange [105] ($-0.00062\langle r^2 \rangle$ meV). Similar results have been obtained by Pachucki [12] and Karshenboim [76]. Indelicato has also re-evaluated the main radiative corrections accounting for finite-size effects [78]. He computed the all-order finite-size corrections to the all-order one-loop eVP (one-loop eVP + eVP iteration) and to the Källén-Sabry (including eVP iteration) term, using a dipole charge distribution. Moreover Indelicato and Mohr calculated the finite-size correction to the muon self-energy perturbatively, and confirmed their result by using also an all-order finite-size approach [78, 80]. Finite-size corrections to higher-order radiative contributions are negligible.

The total radiative corrections to finite-size in one-photon exchange (OPE) is given by

$$\Delta E^{\mathrm{rad}}_{\mathrm{OPE}} = -0.0282\langle r^2 \rangle - 0.0002\langle r^2 \rangle + 0.0009\langle r^2 \rangle \ \mathrm{meV} = -0.0275\langle r^2 \rangle \ \mathrm{meV}. \tag{23}$$

The higher-order finite-size correction given in Table II for Borie is $\Delta E^{\mathrm{ho, Borie}}_{\mathrm{finite\ size}} = -0.000123$ meV [77] originating from the terms in Eq. (9) not proportional to $\langle r^2 \rangle$ and $R^3_{(2)}$. For Indelicato the higher-order finite-size correction $\Delta E^{\mathrm{ho, Indelicato}}_{\mathrm{finite\ size}} = 0.00001(10)$ meV (Eq. (114) in [78]) is the sum of the terms in Eq. (22) beyond r^2_{E} and r^3_{E} and the radiative finite-size corrections beyond the $\langle r^2 \rangle$ terms for one-loop eVP, Källén-Sabry and muon self-energy.

6. Summary of finite-size contributions

From Table II we see that the finite-size contributions are (OPE: one-photon exchange, TPE: two-photon exchange)

$$\begin{aligned}
\Delta E_{\text{finite size}}^{\text{th}} &= \Delta E_{\text{OPE}} + \Delta E_{\text{OPE}}^{\text{rad}} + \Delta E_{\text{TPE}} + \Delta E_{\text{TPE,el.}}^{\text{rad}} + \Delta E_{\text{TPE,inel.}}^{\text{rad}} + \Delta E_{\text{finite size}}^{\text{ho}} \\
&= -5.1994\, r_{\text{E}}^2 - 0.0275\, r_{\text{E}}^2 + 0.0332(20) - 0.00062\, r_{\text{E}}^2 + 0.00018 \\
&\quad + 0.00001(10) \text{ meV}.
\end{aligned} \tag{24}$$

Here, ΔE_{OPE} is given by Eq. (13), $\Delta E_{\text{OPE}}^{\text{rad}}$ is from Eq. (23), and ΔE_{TPE} is from Eq. (19), $\Delta E_{\text{TPE,el.}}^{\text{rad}} = -0.00062\, r_{\text{E}}^2$ are radiative corrections to the elastic part of the TPE contribution calculated by Borie [77], $\Delta E_{\text{TPE,inel.}}^{\text{rad}}$ is the sum of eVP (0.00019 meV) and SE (-0.00001 meV) corrections to the (inelastic) proton polarizability [77] (sum of #26 and #27 in Table II), and $\Delta E_{\text{finite size}}^{\text{ho}}$ are higher-order finite size corrections [78]. Each term corresoponds to one block in Table II. In sum we obtain

$$\Delta E_{\text{finite size}}^{\text{th}} = -5.2275(10)\, r_{\text{E}}^2 + 0.0332(20) + 0.0002(1) \text{ meV}. \tag{25}$$

The uncertainty of the r_{E}^2 coefficient accounts for the difference between the all-order and perturbative approach and uncertainties related to the proton charge distribution. Including the contributions summarized in Table I we obtain the total Lamb shift prediction

$$\begin{aligned}
\Delta E_{\text{L}}^{\text{th}} &= 206.0336(15) - 5.2275(10)\, r_{\text{E}}^2 + 0.0332(20) \text{ meV} \\
&= 206.0668(25) - 5.2275(10)\, r_{\text{E}}^2 \text{ meV}.
\end{aligned} \tag{26}$$

Note that the third Zemach moment or r_{E}^3 contribution has now been accounted for in a more appropriate quantum field framework by the full TPE contribution ΔE_{TPE}. Equation (26) can be compared with the results in Ref. [14]

$$\begin{aligned}
\Delta E_{\text{L}}^{\text{th}} &= 206.0573(45) - 5.2262\, r_{\text{E}}^2 + 0.0347\, r_{\text{E}}^3 \text{ meV} \\
&= 206.0779(45) - 5.2262\, r_{\text{E}}^2 \text{ meV}
\end{aligned} \tag{27}$$

and in Borie-v6

$$\begin{aligned}
\Delta E_{\text{L}}^{\text{th}} &= 206.0592(60) - 5.2272\, r_{\text{E}}^2 + 0.0365(18)\, r_{\text{E}}^3 \text{ meV} \\
&= 206.0808(61) - 5.2272\, r_{\text{E}}^2 \text{ meV}.
\end{aligned} \tag{28}$$

The difference in the constant terms between Eq. (26) and Eqs. (27) and (28) originates mainly from item #18 in Table II (0.013 meV) which was double-counted in Ref. [14]. Another double counting in Ref. [14] was related to #21 and #12. The uncertainty of the proton structure independent term in Eq. (26) is given mainly by the uncertainties of the radiative-recoil correction #24 and uncalculated higher-order terms.

IV.   2S-HFS AND THE ZEMACH RADIUS

The interaction between the bound particle and the magnetic field induced by the magnetic moment of the nucleus gives rise to shifts and splittings of the energy levels termed hyperfine effects. In classical electrodynamics the interaction between the magnetic moments $\boldsymbol{\mu}_p$, and $\boldsymbol{\mu}_\mu$ of proton and muon, respectively, is described by [72]

$$H_{\text{HFS}}^{\text{classical}} = -\frac{2}{3}\boldsymbol{\mu}_p \cdot \boldsymbol{\mu}_\mu \delta(\boldsymbol{r}) \tag{29}$$

where $\delta(\boldsymbol{r})$ is the delta-function in coordinate space. A similar Hamiltonian can be derived in quantum field theory from the one-photon exchange diagram. Using the Coulomb wave function this gives rise in first order perturbation theory to an energy shift for muonic hydrogen nS-states of [77]

$$
\begin{aligned}
E_{\text{HFS}}(F) &= \frac{4(Z\alpha)^4 m_r^3}{3n^3 m_\mu m_p}(1+\kappa)(1+a_\mu)\frac{1}{2}\left[F(F+1)-\frac{3}{2}\right] \\
&= \Delta E_{\text{Fermi}}\frac{1}{2}\left[F(F+1)-\frac{3}{2}\right]
\end{aligned}
\tag{30}
$$

where $\Delta E_{\text{Fermi}} = 22.8320$ meV[77] is the Fermi energy, m_p the proton mass, F the total angular momentum, κ and a_μ the proton and muon anomalous magnetic moments, respectively. The $F=1$ state is shifted by $1/4 \times 22.8320$ meV whereas the $F=0$ state by $-3/4 \times 22.8320$ meV (see Fig. 1). Equation (30) accounts for the sum of the terms (h1) and (h4) in Table III. The Breit term (h2) corrects for relativistic and binding effects accounted for in the Dirac-Coulomb wave function, but excluded in the Schrödinger wave function.

Table III also summarizes the corrections arising from QED, recoil, nuclear structure, hadronic and weak interaction effects. The structure-dependent corrections, scaling as the reduced mass of the system, become large in μp compared to hydrogen. The largest correction is thus given by finite-size effect which, in the non-relativistic limit, is given by the well known Zemach term (h20) [94, 106]

$$\Delta E_{\text{Zemach}} = -\Delta E_{\text{Fermi}} \cdot 2(Z\alpha)m_r \, r_{\text{Z}} \tag{31}$$

where r_{Z} is the Zemach radius defined as

$$r_{\text{Z}} = \int \mathrm{d}^3 r \int \mathrm{d}^3 r' \, r \, \rho_E(\boldsymbol{r})\rho_M(\boldsymbol{r}-\boldsymbol{r}') \tag{32}$$

with ρ_M and ρ_E being the normalized proton magnetization and charge distributions, respectively. The convolution between charge and magnetization distribution in r_{Z} is a consequence of the interaction of the proton spin distributed spatially (given by the magnetic form factor) with the spatial distribution of the muon spin which is described by the atomic muon wave function. The latter is slightly affected, notably at the origin, by the charge-finite-size effect and thus by ρ_E. In a quantum field framework this contribution arises from two-photon exchange processes. Similar to the situation for the Lamb shift discussed above, the intermediate virtual proton may be either "on-shell" or "off-shell". Hence polarizability contributions need to be accounted for (h22). This

term has the largest uncertainty. It arises from the uncertainty of the polarized structure functions g_1 [107, 108] and g_2 [109] (measured in inelastic polarized electron-proton scattering) needed as an input to calculate this contribution. For the HFS (in contrast to the Lamb shift) no subtraction term is required for the calculation of the two-photon exchange diagrams via Compton scattering and dispersion analysis [110].

The leading recoil correction to the HFS (h23) is generated by the same two-photon exchange diagram and is of order $(Z\alpha)(m/M)\tilde{E}_{\text{Fermi}}$ where $\tilde{E}_{\text{Fermi}}$ is the Fermi energy without contribution of the muon anomalous magnetic moment [72].

Radiative corrections which are not accounted for by the anomalous magnetic moment are listed separately in Tab. III. The largest radiative correction is related to the distortion of the wave functions caused by the Uehling potential, items (h5), (h7), (h11) and (h25). Other corrections account for modifications of the magnetic interaction caused by the eVP in one- and two-photon exchange (h8), (h9) and (h10), and vertex corrections caused mainly by the muon self-energy (h13) and (h14).

The main HFS contributions have been confirmed and refined by Indelicato [78] by numerical integration of the hyperfine Hamiltonian with Bohr-Weisskopf (magnetization distribution) correction using Dirac wave functions. The latter have been calculated for Coulomb finite-size and Uehling potentials. All-order finite-size, relativistic and eVP effects are thus included in the wave function. This calculation is performed for various r_E and r_Z, assuming exponential charge and magnetization distributions. From these calculations the terms (h3), (h6), (h20), (h21) and (h25) are obtained, showing good agreement with the perturbative results. It is interesting to note that the HFS shows a small dependence on r_E^2 given by the term (h21). The small constant terms in (h21) and (h25) account for the sum of higher order terms of a polynomial expansion in r_E and r_Z (r_Z^2, $r_E r_Z$, $r_E^2 r_Z$, $r_E r_Z^2$, $r_E^2 r_Z^2$ etc.) of the numerical results obtained in [78].

The sum of all contributions in Table III is

$$\Delta E_{\text{HFS}}^{\text{th}} = 22.9763(15) - 0.1621(10)r_Z + \Delta E_{\text{HFS}}^{\text{pol}} \text{ meV} \tag{33}$$

where r_Z is in fm. Using the value $\Delta E_{\text{HFS}}^{\text{pol}} = 0.0080(26)$ meV [115] results in

$$\Delta E_{\text{HFS}}^{\text{th}} = 22.9843(30) - 0.1621(10)r_Z \text{ meV}. \tag{34}$$

The uncertainty of the first term in Eq. (33) considers differences between results from various authors and uncalculated higher-order terms.

V. CONCLUSIONS

We have presented an update of the theoretical predictions for the 2S Lamb shift in muonic hydrogen (see Eq. (26))

$$\begin{aligned} \Delta E_L^{\text{th}} &= 206.0336(15) - 5.2275(10)\, r_E^2 + 0.0332(20) \text{ meV} \\ &= 206.0668(25) - 5.2275(10)\, r_E^2 \text{ meV}. \end{aligned} \tag{35}$$

TABLE III: All known contributions to the 2S-HFS in μp from different authors, and the one we selected (usually the all-order calculations which we consider more complete). Values are in meV, radii in fm. SE: self-energy, VP: vacuum polarization, Rel: relativistic, RC: recoil correction, PT: perturbation theory, p: proton, int: interaction, AMM: anomalous magnetic moment.

	Contribution	Martynenko [70]	Borie-v6 [77]	Indelicato [78]	Our choice	Ref.
h1	Fermi energy, $(Z\alpha)^4$	22.8054	22.8054			
h2	Breit corr., $(Z\alpha)^6$	0.0026	0.00258			
h3	Dirac energy (+ Breit corr. in all-order)			22.807995	22.807995	Eq. (107) in [78]
h4	μ AMM corr., $\alpha(Z\alpha)^4$, $\alpha(Z\alpha)^4$	0.0266	0.02659		0.02659	
h5	eVP in 2nd-order PT, $\alpha(Z\alpha)^5$ ($\epsilon_{\rm VP2}$)	0.0746	0.07443			
h6	All-order eVP corr.			0.07437	0.07437	Eq. (109) in [78]
h7	Two-loop corr. to Fermi-energy ($\epsilon_{\rm VP2}$)		0.00056		0.00056	
h8	One-loop eVP in 1γ int., $\alpha(Z\alpha)^4$ ($\epsilon_{\rm VP1}$)	0.0482	0.04818		0.04818	
h9	Two-loop eVP in 1γ int., $\alpha^2(Z\alpha)^4$ ($\epsilon_{\rm VP1}$)	0.0003	0.00037		0.00037	
h10	Further two-loop eVP corr.		0.00037		0.00037	[111, 112]
h11	μVP (similar to $\epsilon_{\rm VP2}$)		0.00091		0.00091	
h12	μVP (similar to $\epsilon_{\rm VP1}$)	0.0004	(incl. in h13)		(incl. in h13)	
h13	Vertex, $\alpha(Z\alpha)^5$		-0.00311		-0.00311	[a]
h14	Higher order corr. of (h13), (part with $\ln(\alpha)$)		-0.00017		-0.00017	[113]
h15	μ SE with p structure, $\alpha(Z\alpha)^5$	0.0010				
h16	Vertex corr. with proton structure, $\alpha(Z\alpha)^5$	-0.0018				
h17	"Jellyfish" corr. with p structure, $\alpha(Z\alpha)^5$	0.0005				
h18	Hadron VP, α^6	0.0005(1)	0.00060(10)		0.00060(10)	
h19	Weak interaction contribution	0.0003	0.00027		0.00027	[114]
h20	Finite-size (Zemach) corr. to $\Delta E_{\rm Fermi}$, $(Z\alpha)^5$	-0.1518^b	-0.16037 $r_{\rm Z}$	-0.16034 $r_{\rm Z}$	-0.16034 $r_{\rm Z}$	Eq. (107) in [78]
h21	Higher-order finite-size corr. to $\Delta E_{\rm Fermi}$			-0.0022 $r_{\rm E}{}^2$ +0.0009	-0.0022 $r_{\rm E}{}^2$ +0.0009	Eq. (107) in [78]
h22	Proton polarizability, $(Z\alpha)^5$, $\Delta E_{\rm HFS}^{\rm pol}$	0.0105(18)	0.0080(26)		0.00801(260)	[115, 116]
h23	Recoil corr.	(incl. in h20)	0.02123		0.02123	[110]
h24	eVP + proton structure corr., α^6	-0.0026				
h25	eVP corr. to finite-size (similar to $\epsilon_{\rm VP2}$)		-0.00114	-0.0018 $r_{\rm Z}$ -0.0001	-0.0018 $r_{\rm Z}$ -0.0001	Eq. (109) in [78]
h26	eVP corr. to finite-size (similar to $\epsilon_{\rm VP1}$)		-0.00114		-0.00114(20)	
h27	Proton structure corr., $\alpha(Z\alpha)^5$	-0.0017				
h28	Rel. + radiative RC with p AMM, α^6	0.0018				
	Sum	$22.8148(20)^c$	22.9839(26) -0.1604 $r_{\rm Z}$		22.9858(26) -0.1621(10) $r_{\rm Z}$ - 0.0022(5) $r_{\rm E}^2$	
	Sum with $r_{\rm E}$ = 0.841 fm, $r_{\rm Z}$ = 1.045 fm [28]	22.8148 meV	22.8163 meV		22.8149 meV	

[a]Includes a correction $\alpha(Z\alpha)^5$ due to μVP.
[b]Calculated using the Simon et al. form factor.
[c]The uncertainty is 0.0078 meV if the uncertainty of the Zemach term (h20) is included (see Table II of [70]).

Similarly, the 2S hyperfine splitting (HFS) in muonic hydrogen is (see Eq. (33))

$$\Delta E_{\rm HFS}^{\rm th} = 22.9763(15) - 0.1621(10)r_{\rm Z} + 0.0080(26) \text{ meV}$$
$$= 22.9843(30) - 0.1621(10)r_{\rm Z} \text{ meV}.$$

(36)

Double-counting of a few higher-order terms in previous compilations has been eliminated. No large error and no missing contributions beyond 0.001 meV have been found. Finite-size and one-

loop eVP has recently been studied also by numerical integration of the Dirac equation including the finite-size Coulomb potential and Uehling potential [78], confirming the perturbative results, for both the Lamb shift and the HFS. The uncertainty arising from the two-photon exchange is still debated but large contributions seem unlikely. The total unertainty of the Lamb shift theory has been reduced by a factor of 2 since the summary [14].

The 0.3 meV (7σ) discrepancy between the proton rms charge radii $r_{\rm E}$ from muonic hydrogen [1, 2] and CODATA-2010 [15] persists. The "proton radius puzzle" remains.

VI. ACKNOWLEDGMENTS

[1] R. Pohl, A. Antognini, F. Nez, F. D. Amaro, F. Biraben, J. M. R. Cardoso, D. S. Covita, A. Dax, S. Dhawan, L. M. P. Fernandes, et al., Nature **466**, 213 (2010).

[2] A. Antognini, F. Nez, K. Schuhmann, F. D. Amaro, F. Biraben, J. M. R. Cardoso, D. S. Covita, A. Dax, S. Dhawan, M. Diepold, et al., submitted (2012).

[3] C. G. Parthey, A. Matveev, J. Alnis, B. Bernhard, A. Beyer, R. Holzwarth, A. Maistrou, R. Pohl, K. Predehl, T. Udem, et al., Phys. Rev. Lett. **107**, 203001 (2011), [arXiv: 1107.3101 (atom-ph)].

[4] B. de Beauvoir, C. Schwob, O. Acef, L. Jozefowski, L. Hilico, F. Nez, L. Julien, A. Clairon, and F. Biraben, Eur. Phys. J. D **12**, 61 (2000).

[5] S. Chu, A. P. Mills, A. G. Yodh, K. Nagamine, Y. Miyake, and T. Kuga, Phys. Rev. Lett. **60**, 101 (1988).

[6] K. Danzmann, M. S. Fee, and S. Chu, Phys. Rev. A **39**, 6072 (1989).

[7] D. Hanneke, S. Fogwell, and G. Gabrielse, Phys. Rev. Lett. **100**, 120801 (2008).

[8] S. Sturm, A. Wagner, B. Schabinger, J. Zatorski, Z. Harman, W. Quint, G. Werth, C. H. Keitel, and K. Blaum, Phys. Rev. Lett. **107**, 023002 (2011).

[9] S. G. Karshenboim, Phys. Rep. **422**, 1 (2005).

[10] U. D. Jentschura, P. J. Mohr, J. N. Tan, and B. J. Wundt, Phys. Rev. Lett. **100**, 160404 (2008).

[11] K. Pachucki, Phys. Rev. A **53**, 2092 (1996).

[12] K. Pachucki, Phys. Rev. A **60**, 3593 (1999).

[13] E. Borie, Phys. Rev. A **71**, 032508 (2005).

[14] R. Pohl, A. Antognini, F. Nez, F. D. Amaro, F. Biraben, J. M. R. Cardoso, D. S. Covita, A. Dax, S. Dhawan, L. M. P. Fernandes, et al., Supplementary information to Nature **466**, 213 (2010), URL http://www.nature.com/nature/journal/v466/n7303/extref/nature09250-s1.pdf.

[15] P. J. Mohr, B. N. Taylor, and D. B. Newell, Rev. Mod. Phys. **84**, 1527 (2012), [arXiv: 1203.5425 (physics.atom-ph)].

[16] S. R. Lundeen and F. M. Pipkin, Phys. Rev. Lett. **46**, 232 (1981).

[17] E. W. Hagley and F. M. Pipkin, Phys. Rev. Lett. **72**, 1172 (1994).

[18] C. Schwob, L. Jozefowski, B. de Beauvoir, L. Hilico, F. Nez, L. Julien, F. Biraben, O. Acef, J.-J. Zondy, and A. Clairon, Phys. Rev. Lett. **82**, 4960 (1999).

[19] M. Fischer, N. Kolachevsky, M. Zimmermann, R. Holzwarth, T. Udem, T. W. Hänsch, M. Abgrall, J. Grünert, I. Maksimovic, S. Bize, et al., Phys. Rev. Lett. **92**, 230802 (2004).

[20] C. G. Parthey, A. Matveev, J. Alnis, R. Pohl, T. Udem, U. D. Jentschura, N. Kolachevsky, and T. W. Hänsch, Phys. Rev. Lett. **104**, 233001 (2010).

[21] O. Arnoult, F. Nez, L. Julien, and F. Biraben, Eur. Phys. J. D **60**, 243 (2010).

[22] I. Sick, Phys. Lett. B **576**, 62 (2003).

[23] P. G. Blunden and I. Sick, Phys. Rev. C **72**, 057601 (2005).

[24] J. C. Bernauer, P. Aschenbach, C. Ayerbe Gayoso, R. Böhm, D. Bosnar, L. Debenjak, M. O. Distler, L. Doria, A. Esser, et al., Phys. Rev. Lett. **105**, 242001 (2010), [arXiv: 1007.5076 (nucl-ex)].

[25] R. Pohl, A. Antognini, F. Nez, F. D. Amaro, F. Biraben, J. M. R. Cardoso, D. S. Covita, A. Dax, S. Dhawan, L. M. P. Fernandes, et al., Can. J. Phys. **89**, 37 (2010).

[26] U. D. Jentschura, Ann. Phys. **326**, 516 (2011).

[27] J.-P. Karr and L. Hilico, Phys. Rev. Lett. **109**, 103401 (2012), [arXiv:1205.0633 (physics.atom-ph)].

[28] M. O. Distler, J. C. Bernauer, and T. Walcher, Phys. Lett. B **696**, 343 (2011).

[29] X. Zhan, K. Allada, D. S. Armstrong, J. Arrington, W. Bertozzi, W. Boeglin, et al., Phys. Lett. B **705**, 59 (2011).

[30] I. C. Cloet and G. A. Miller, Phys. Rev. C **83**, 012201(R) (2011).

[31] R. J. Hill and G. Paz, Phys. Rev. D **82**, 113005 (2010).

[32] G. Ron, X. Zhan, J. Glister, B. Lee, K. Allada, W. Armstrong, J. Arrington, A. Beck, F. Benmokhtar, B. L. Berman, et al. (The Jefferson Lab Hall A Collaboration), Phys. Rev. C **84**, 055204 (2011).

[33] D. K. Hasell, R. G. Milner, R. P. Redwine, R. Alarcon, H. Gao, M. Kohl, and J. Calarco, Ann. Rev. Nucl. Part. Sci. **61**, 409 (2011).

[34] I. Sick, Few-Body Syst. **50**, 367 (2011).

[35] S. Gilad, Few-Body Systems **50**, 451 (2011).

[36] C. Adamuscin, S. Dubnicka, and A. Z. Dubnickova, Nucl. Phys. B, (Proc. Suppl.) **219-220**, 178 (2011).

[37] C. Adamuscin, S. Dubnicka, and A. Z. Dubnickova, Prog. Part. Nucl. Phys. **67**, 479 (2012).

[38] I. Sick, Prog. Part. Nucl. Phys. **67**, 473 (2012).

[39] U. Müller, Progress in Particle and Nuclear Physics **67**, 607 (2012).

[40] A. Pineda, Phys. Rev. C **71**, 065205 (2005).

[41] M. Vanderhaeghen and T. Walcher, Nucl. Physics News **21**, 14 (2010), arXiv: 1008.4225.

[42] G. A. Miller, A. W. Thomas, J. D. Carroll, and J. Rafelski, Phys. Rev. A **84**, 020101(R) (2011), [arXiv: 1101.4073 (physics.atom-ph)].

[43] R. J. Hill and G. Paz, Phys. Rev. Lett. **107**, 160402 (2011).

[44] P. Hägler, Prog. Theo. Phys. Suppl. **187**, 221 (2011).

[45] S. Collins, M. Gockeler, P. Hagler, R. Horsley, Y. Nakamura, et al., Phys.Rev. **D84**, 074507 (2011).

[46] M. C. Birse and J. A. McGovern, Eur. Phys. J. A **48**, 120 (2012), [arXiv: 1206.3030 (hep-ph)].

[47] I. T. Lorenz, H.-W. Hammer, and U.-G. Meissner, Eur. Phys. J. A **48**, 151 (2012), [arXiv: 1205.6628 (hep-ph)].

[48] T. Ledwig, J. Martin-Camalich, V. Pascalutsa, and M. Vanderhaeghen, Phys. Rev. D **85**, 034013 (2012).

[49] P. Brax and C. Burrage, Phys. Rev. D **83**, 035020 (2011).

[50] J. I. Rivas, A. Camacho, and E. Göklü, Phys. Rev. D **84**, 055024 (2011).

[51] S. G. Karshenboim, Phys. Rev. Lett. **104**, 220406 (2010).

[52] J. Jaeckel and S. Roy, Phys. Rev. D **82**, 125020 (2010).

[53] V. Barger, C.-W. Chiang, W.-Y. Keung, and D. Marfatia, Phys. Rev. Lett. **106**, 153001 (2011).

[54] D. Tucker-Smith and I. Yavin, Phys. Rev. D **83**, 101702 (2011).

[55] B. Batell, D. McKeen, and M. Pospelov, Phys. Rev. Lett. **107**, 011803 (2011), [arXiv: 1103.0721 (hep-ph)].

[56] V. Barger, C.-W. Chiang, W.-Y. Keung, and D. Marfatia, Phys. Rev. Lett. **108**, 081802 (2012).

[57] D. McKeen and M. Pospelov, Phys. Rev. Lett. **108**, 263401 (2012).

[58] C. E. Carlson and B. C. Rislow, Phys. Rev. D **86**, 035013 (2012), [arXiv: 1206.3587v2 (hep-ph)].

[59] J. L. Flowers, P. E. G. Baird, L. Bougueroua, H. A. Klein, and H. S. Margolis, IEEE Trans. Instrum. Meas. **56**, 331 (2007).

[60] J. N. Tan, S. M. Brewer, and N. D. Guise, Phys. Scr. T **144**, 014009 (2011).

[61] F. Biraben, Eur. Phys. J. Special Topics **172**, 109 (2009), [arXiv: 0809.2985 (atom-ph)].

[62] E. A. Hessels, *private communication* (2012).

[63] M. Kohl, AIP Conf. Proc. **1160**, 19 (2009).

[64] P. Balakrishnan et al., *A Proposal for the DarkLight Jefferson Lab: High Precision Measurement of the Proton Charge Radius* (2010).

[65] A. Gasparian et al., *Proposal to Jefferson Lab PAC-38: High Precision Measurement of the Proton Charge Radius* (2011).

[66] B. A. Raue, AIP Conf. Proc. **1257**, 617 (2010).

[67] K. Slifer, AIP Conf. Proc. **1432**, 118 (2012).

[68] A. Adamczak, D. Bakalov, L. Stoychev, and A. Vacchi, Nucl. Inst. Meth. **B281**, 72 (2012).

[69] A. Antognini, F. Nez, F. D. Amaro, F. Biraben, J. M. R. Cardoso, D. S. Covita, A. Dax, S. Dhawan, L. M. P. Fernandes, A. Giesen, et al., Can. J. Phys. **89**, 47 (2010).

[70] A. P. Martynenko, Phys. Rev. A **71**, 022506 (2005).

[71] A. P. Martynenko, Physics of Atomic Nuclei **71**, 125 (2008).

[72] M. I. Eides, H. Grotch, and V. A. Shelyuto, Phys. Rep. **342**, 63 (2001).

[73] M. I. Eides, H. Grotch, and V. A. Shelyuto, *Theory of Light Hydrogenlike Atoms* (Springer Tracts in Modern Physics **222**, 2006).

[74] U. D. Jentschura, Ann. Phys. **326**, 500 (2011).

[75] U. D. Jentschura, Phys. Rev. A **84**, 012505 (2011).

[76] S. G. Karshenboim, V. G. Ivanov, and E. Y. Korzinin, Phys. Rev. A **85**, 032509 (2012).

[77] E. Borie, Ann. Phys. **327**, 733 (2012), and arXiv: 1103.1772-v6.

[78] P. Indelicato, arXiv 1210.5828v2 (physics.atom-ph) (2012).

[79] J. D. Carroll, A. W. Thomas, J. Rafelski, and G. A. Miller, Phys. Rev. A **84**, 012506 (2011).

[80] P. Indelicato and P. J. Mohr, to be submitted (2012).

[81] S. Romanov, Z. Phys. D **33**, 17 (1995).

[82] J. D. Carroll, A. W. Thomas, J. Rafelski, and G. A. Miller, arXiv:1108.2541v1 (2011).

[83] U. D. Jentschura and B. J. Wundt, Eur. Phys. J. D **65**, 357 (2011).

[84] E. Borie and G. A. Rinker, Rev. Mod. Phys. **54**, 67 (1982).

[85] V. G. Ivanov, E. Y. Korzinin, and S. G. Karshenboim, Phys. Rev. D **80**, 027702 (2009).

[86] T. Kinoshita and M. Nio, Phys. Rev. Lett. **82**, 3240 (1999).

[87] S. G. Karshenboim, E. Y. Korzinin, V. G. Ivanov, and V. A. Shelyuto, JETP Lett. **92**, 8 (2010).

[88] R. Barbieri, M. Caffo, and E. Remiddi, Lett. Nuovo Cimento **7**, 60 (1963).

[89] H. Suura and E. H. Wichmann, Phys. Rev. **105**, 1930 (1957).

[90] A. Petermann, Phys. Rev. **105**, 1931 (1957).

[91] J. Friar, J. Martorell, and D. Sprung, Phys. Rev. A **59**, 4061 (1999).

[92] A. P. Martynenko and R. Faustov, Physics of Atomic Nuclei **63**, 845 (2000).

[93] A. P. Martynenko and R. Faustov, Physics of Atomic Nuclei **64**, 1282 (2001).

[94] J. L. Friar, Ann. Phys. **122**, 151 (1979).

[95] J. L. Friar and I. Sick, Phys. Rev. A **72**, 040502 (2005).

[96] A. De Rújula, Phys. Lett. B **693**, 555 (2011).

[97] A. De Rújula, Phys. Lett. B **697**, 26 (2011).

[98] A. Pineda, PoS **QNP2012**, 002 (2012), Sixth International Conference on Quarks and Nuclear Physics, April 16-20, 2012, Ecole Polytechnique, Palaiseau, Paris, URL `http://pos.sissa.it/archive/conferences/157/002/QNP2012_002.pdf`.

[99] C. E. Carlson and M. Vanderhaeghen, Phys. Rev. A **84**, 020102 (2011).

[100] A. P. Martynenko, Physics of Atomic Nuclei **69**, 1309 (2006), [arXiv: hep-ph/0509236].

[101] G. A. Miller, A. W. Thomas, and J. D. Carroll, arXiv:1207.0549 (2012).

[102] J. J. Kelly, Phys. Rev. C **70**, 068202 (2004).

[103] J. Arrington, W. Melnitchouk, and J. A. Tjon, Phys. Rev. C **76**, 035205 (2007).

[104] B. Y. Wu and C. W. Kao, arXiv:1108.2968 (2011).

[105] M. I. Eides and H. Grotch, Phys. Rev. A **56**, R2507 (1997).

[106] A. C. Zemach, Phys. Rev. **104**, 1771 (1956).

[107] Y. Prok and other, Physics Letters B **672**, 12 (2009).

[108] P. Anthony, R. Arnold, T. Averett, H. Band, M. Berisso, H. Borel, P. Bosted, S. Bültmann, M. Buenerd, T. Chupp, et al., Physics Letters B **493**, 19 (2000).

[109] F. R. Wesselmann, K. Slifer, S. Tajima, A. Aghalaryan, A. Ahmidouch, R. Asaturyan, F. Bloch, W. Boeglin, P. Bosted, C. Carasco, et al. (Resonance Spin Structure Collaboration), Phys. Rev. Lett. **98**, 132003 (2007).

[110] C. E. Carlson, V. Nazaryan, and K. Griffioen, Phys. Rev. A **78**, 022517 (2008).

[111] S. G. Karshenboim, E. Y. Korzinin, and V. G. Ivanov, JETP Lett. **88**, 641 (2008).

[112] S. G. Karshenboim, E. Y. Korzinin, and V. G. Ivanov, JETP Lett. **89**, 216 (2009).

[113] S. J. Brodsky and G. W. Erickson, Phys. Rev. **148**, 26 (1966).

[114] M. I. Eides, Phys. Rev. A **85**, 034503 (2012).

[115] C. E. Carlson, V. Nazaryan, and K. Griffioen, Phys. Rev. A **83**, 042509 (2011).

[116] E. Cherednikova, R. Faustov, and A. Martynenko, Nucl. Phys. A **703**, 365 (2002).